

Proton fragmentation functions considering finite-mass corrections

S. M. Moosavi Nejad^{a,b,*}, M. Soleymaninia^{c,†} and A. Maktoubian^a

^(a) *Faculty of Physics, Yazd University, P.O.Box 89195-741, Yazd, Iran*

^(b) *School of Particles and Accelerators, Institute for Research in Fundamental Sciences (IPM), P.O.Box 19395-5531, Tehran, Iran*

^(c) *Islamic Azad University, North Tehran Branch, Tehran, Iran*

(Dated: September 7, 2018)

We present new sets of proton fragmentation functions describing the production of protons from the gluon and each of the quarks, obtained by a global fit to all relevant data sets extracted from the single-inclusive electron-positron annihilation. Our analysis is in good agreement with e^+e^- annihilation data. We also impose the finite-mass effects of proton in our calculations, a topic with a very little attention paid to in the literatures. Proton mass effects turn out to be appreciable for the gluon and light quark fragmentation functions, so the inclusion of finite-mass effects tends to improve the overall description of the data by reducing the minimized χ^2 values, significantly. As an application, we also apply the extracted fragmentation functions to make our predictions for the scaled-energy distribution of protons inclusively produced in top quark decays at next-to-leading order, relying on the universality and scaling violations of fragmentation functions.

PACS numbers: 13.87.Fh, 13.66.Bc, 13.60.Hb, 13.85.Ni

I. INTRODUCTION

The mechanism of hadronization is explained by the fragmentation function (FF), so that the FFs are the key quantities for calculating the hadroproduction cross sections. The FFs $D_i^H(z, \mu_F^2)$ can be described as the fragmenting probability of a parton i at the factorization scale μ_F into a hadron H carrying away a fraction z of its momentum. For this respect, one needs to determine these functions with higher accuracy so that, recently, in [1] using the data from e^+e^- annihilation an analysis of the pion fragmentation functions (FFs) is studied at next-to-next-to-leading order (NNLO). The specific importance of FFs is for their model-independent predictions of the cross sections at the Large Hadron Collider (LHC). Specifically, one of the proposed channels to study the properties of top quarks at the LHC is to consider the energy spectrum of outgoing mesons from top decays. In this way, by having parton-level differential decay rates [2–4] and the FFs of partons into hadrons, one calculates the energy spectrum of mesons observed. For example, CMS Collaboration reconstructs the top mass from the peak of B-hadron energy [5, 6]. Since the hadroproduction mechanism is universal and independent of the perturbative process which produces partons, one can extract, for example, the existing data on $e^+e^- \rightarrow b\bar{b} \rightarrow H + jets$ events to fit the proposed models for the transition $b \rightarrow H$, and describe the b-quark non-perturbative fragmentation in each other process, such as top decay $t \rightarrow W^+(\rightarrow l^+\nu_l) + b(\rightarrow H)$. Interests in FFs are also in, for example, tests of QCD such as theoretical calculations for recent measurements of inclusive produc-

tion in proton-proton collisions at the Relativistic Heavy Ion Collider (RHIC), and in investigating the origin of the proton spin.

Commonly, two main schemes are applied to evaluate the FFs. The first scheme is based on the fact that the FFs for hadrons containing a heavy quark or antiquark are analytically calculable by virtue of perturbative QCD (pQCD) [7, 8]. The first theoretical attempt to illustrate the procedure of heavy hadroproduction was made by Bjorken [9] by employing a naive quark-parton model. Bjorken deduced that the inclusive energy distribution of heavy hadrons should peak almost at $x_H = 1$, where x_H stands for the scaled-energy variable of hadrons. The perturbative QCD scheme was followed by Peterson [10], Suzuki [11], Amiri and Ji [12], while in this scheme Suzuki calculates the heavy FFs by using a convenient Feynman diagram and considering a typical wave function for the hadronic bound states. In [13], using the Suzuki's model we calculated the FF for a charm quark to split into S-wave D^0/D^+ mesons at the initial scale $\mu_F = m_D$, and our result for the initial FF of gluon to split into S-wave charmonium states ($\eta_c, J/\psi$) to leading order in the QCD coupling constant α_s is presented in [14].

In a more reliable scheme, which is frequently used to obtain the FFs, these functions are parametrized in a specific model with some free parameters so that these parameters are determined from experimental data analysis using the data from e^+e^- reactions, lepton-hadron and hadron-hadron scattering processes. This scheme is in similarity with the approach used for determination of the parton distribution functions (PDFs)[15]. Among all scattering processes, the e^+e^- annihilation processes provide a whole clean environment to determine the FFs, however, without an initial hadron state one can not separate quark distributions from antiquark distributions. There are several phenomenological studies on QCD analysis of fragmentation functions which used spe-

*Electronic address: mmoosavi@yazd.ac.ir

†Electronic address: maryam_soleymaninia@ipm.ir

cial parametrizations and different experimental data in their global analysis. Recent extracted FFs for light hadrons are related to AKK [16], LSS [17], DSEHS [18], SKMA [19, 20], DSS [21, 22] and HKNS [23] Collaborations who used different phenomenological models and various experimental data. In [19, 20], we determined the π^\pm and K^\pm FFs, at next-to-leading order (NLO) through a global fit to the single-inclusive e^+e^- annihilation (SIA) data and the semi-inclusive deep inelastic scattering asymmetry data from HERMES and COMPASS. There, we broke the symmetry assumption between the quark and antiquark FFs for favored partons by using the asymmetry data.

In this paper, we present a new functional form of proton FFs up to NLO, obtained through a global fit to SIA data from LEP (ALEPH and DELPHI Collaborations), SLAC (SLD and TPC Collaborations) and DESY (TASSO Collaboration) [24–29]. We also impose the effects of proton mass on the FFs, a topic with a very little attention paid to in the literatures, e.g. [21–23]. We show that this effect is important in calculation of the gluon and light quark FFs, specifically in low energies, so this effect reduces the minimized χ^2 and makes a more convenient fit.

In the Standard Model (SM) theory, the top quark has short lifetime so that it decays before hadronization takes place, then the full polarization content of the t -quark is preserved during its decay. Since, one of the channels for studying the top properties is to consider the energy distribution of hadrons inclusively produced in top decays, then we make our predictions for the scaled-energy distribution of protons inclusively produced in top quark decays, $t \rightarrow W^+ + b(\rightarrow p + X)$, using the extracted FFs in our analysis. These distributions will also enable us to deepen our understanding of the non-perturbative aspects of proton formation by hadronization and to pin down the proton FFs. Recently, the local CMS group started to work on a determination of the top quark mass from a detailed study of the produced hadron decays, e.g. the energy peak of bottom-flavored hadrons (B) [5, 6].

This paper is organized as follows. In section II we describe our formalism and parametrization forms for proton fragmentation functions at LO and NLO. Using the SIA data we present our results and shall compare our results with other collaborations. In section III, we explain how to impose the effect of hadron mass on the FFs and compare our results in both cases. Our predictions for the energy spectrum of proton produced in unpolarized top quark decays are presented in section IV. Our conclusion is summarized in section V.

II. QCD ANALYSIS OF PROTON FRAGMENTATION FUNCTIONS

The fragmentation functions are the nonperturbative part of the hadronization processes and have an important and fundamental role in the calculation of single-

inclusive hadron production in any reaction. According to the factorization theorem of the QCD parton model [30], the leading twist component of any single hadron production measurement might be remarked as the convolution of FFs with the equivalent productions of on-shell partons, up to possible PDFs to account for any hadrons in the initial state. Generally, the inclusive production of hadron H in the typical scattering process of $A + B \rightarrow H + X$, can be expressed as

$$d\sigma = \sum_{a,b,c} \int_0^1 dx_a \int_0^1 dx_b \int_0^1 dz f_{a/A}(x_a, Q) f_{b/B}(x_b, Q) \times d\hat{\sigma}(a + b \rightarrow c + X) D_{c \rightarrow H}(z, Q), \quad (1)$$

where a and b are incident partons in the colliding initial hadrons A and B , respectively, $f_{a/A}$ and $f_{b/B}$ are the PDFs at the scale Q^2 of the partonic subprocess $a + b \rightarrow c + X$, c is the fragmenting parton (either a gluon or a quark) and X refers to the unobserved jets. In (1), $D_{c \rightarrow H}(z, Q)$ is the FF at the factorization scale $\mu_F^2 = Q^2$ which can be obtained by evolving from the initial FF $D_{c \rightarrow H}(z, \mu_0)$ using the DGLAP equations [31]. One of the most current ways to specify the FFs is based on the single-inclusive hadroproduction data through electron-positron annihilation, because one does not need to deal with the uncertainty introduced by PDFs which appears in the hadron collisions. From the factorization theorem, the cross section for the e^+e^- annihilation can be expressed in terms of the partonic hard scattering cross sections, which are perturbatively calculable, and the FFs D_i^H , i.e.

$$\frac{1}{\sigma_{tot}} \frac{d}{dx_H} \sigma(e^+e^- \rightarrow HX) = \sum_i C_i(x_H, \alpha_s) \otimes D_i^H(x_H, Q^2), \quad (2)$$

where, σ_{tot} is the total partonic cross section at NLO [32], X stands for the unobserved jets and $D_i^H(x_H, Q^2)$ shows the probability to find the hadron H from a parton $i (= g, u/\bar{u}, d/\bar{d}, \dots)$ with the scaled-energy fraction $x_H = 2E_H/\sqrt{s}$ and C_i 's are the Wilson coefficient functions based on the hard scattering cross section $e^+e^- \rightarrow q\bar{q}$ [33–35]. Also, the convolution integral is defined as $f(z) \otimes g(z) = \int_z^1 dy/y f(y)g(z/y)$. In section III, we shall review the factorization theorem in details and then improve the theorem in the presence of hadron mass.

Generally, there are several different strategies to determine the FFs from data analysis, so in the present analysis we apply the massless scheme or zero-mass variable-flavor-number (ZM-VFN) scheme [32], where the mass of heavy quarks are set to zero from the beginning and the non-zero values of the c - and b -quark masses only enter through the initial conditions of the FFs. In this strategy, the number of active flavors increases for scales higher than the flavor thresholds and this scheme works best for high energy scales.

In a phenomenological approach, the fragmentation functions are parametrized in the convenient functional forms at the initial scales μ_0 , which can be different for light and heavy partons. Up to now, many different phenomenological models like Peterson model [10], Power model [36], Cascade model [37] etc., have been developed to describe the fragmentation functions. In the present work, we apply very flexible parametrization form for the proton FFs at NLO, considering SIA data from LEP (*ALEPH* [24] and *DELPHI* [25, 26] Collaborations), SLAC (*SLD* [27] and *TPC* [28] Collaborations) and DESY (*TASSO* [29] Collaboration). The energy scales of the experimental data are from 29 GeV to 91.28 GeV, and most of the precision e^+e^- annihilation data are limited to results from experiments at LEP and SLAC at the energy scale of $Q^2 = M_Z^2$. In the reported data without discrimination of hadron species, authors distinguished between four cases: fragmentation of u, d and s quarks, c quarks only, b quarks only, and all five quark flavors. These classifications are just in the DELPHI and SLD data (see Tables. III, IV and VI). Note that in our global analysis of data sets from the ALEPH experiments we deal with data in the form of $1/N \times dN^p/dx_p$, where N is the number of detected events, and this fraction is corresponding to $1/\sigma_{tot} \times d\sigma^p/dx_p$, where x_p refers to the energy of proton scaled to the beam energy s , i.e. $x_p = 2E_p/\sqrt{s}$.

At the initial scale of the fragmentation (μ_0), our parametrization contains a functional form as

$$D_i^p(z, \mu_0^2) = N_i z^{\alpha_i} (1-z)^{\beta_i} [1 - e^{-\gamma_i z}], \quad (3)$$

which is a convenient form for the light hadrons. Here, $z = E_p/E_i$ (with $i = g, u, \bar{u}, d, \bar{d}, \dots$) is the energy fraction of the parton i which is taken away by the produced proton. In (3), to control the medium z -region and to increase the accuracy of the global fit the term $[1 - e^{-\gamma_i z}]$ is multiplied. The free parameters N_i , α_i , β_i and γ_i in the proposed form are determined by minimizing χ^2 for differential cross section in x -space and their μ evolution is determined by the DGLAP equations [31]. The χ^2 for k data points is denoted by

$$\chi^2 = \sum_{j=1}^k \left(\frac{E_j - T_j}{\sigma_j^E} \right)^2, \quad (4)$$

where, T_j and E_j stand for the theoretical results and experimental values of $1/\sigma_{tot} \times d\sigma^H/dx_H$, respectively, and σ_j^E is the error of the corresponding experimental data. The systematical and statistical errors are involved in σ_j^E . In Tables. III and IV, based on each collaboration the data characteristics, the χ^2 and the χ^2 values per degree of freedom ($\chi^2/d.o.f$) are listed.

According to the partonic structure of protons $p(uud)$, the following assumptions are considered for our calculations

tions

$$\begin{aligned} D_u^p(z, \mu_0^2) &= ND_d^p(z, \mu_0^2) = N_u z^{\alpha_u} (1-z)^{\beta_u} (1 - e^{-\gamma_u z}) \\ D_{\bar{u}}^p(z, \mu_0^2) &= N' D_{\bar{d}}^p(z, \mu_0^2) = N_{\bar{u}} z^{\alpha_{\bar{u}}} (1-z)^{\beta_{\bar{u}}} (1 - e^{-\gamma_{\bar{u}} z}), \\ D_s^p(z, \mu_0^2) &= D_{\bar{s}}^p(z, \mu_0^2) = N'' D_{\bar{u}}^p(z, \mu_0^2) \\ &= N_s z^{\alpha_{\bar{u}}} (1-z)^{\beta_{\bar{u}}} (1 - e^{-\gamma_{\bar{u}} z}), \end{aligned} \quad (5)$$

and for the gluon and heavy quark FFs, we apply a power model as applied by AKK [16], DSS [22] and HKNS [23] collaborations, i.e.

$$\begin{aligned} D_g^p(z, \mu_0^2) &= N_g z^{\alpha_g} (1-z)^{\beta_g}, \\ D_c^p(z, \mu_0^2) &= D_{\bar{c}}^p(z, \mu_0^2) = N_c z^{\alpha_c} (1-z)^{\beta_c}, \\ D_b^p(z, \mu_0^2) &= D_{\bar{b}}^p(z, \mu_0^2) = N_b z^{\alpha_b} (1-z)^{\beta_b}. \end{aligned} \quad (6)$$

In the assumptions above, we considered the isospin symmetry for sea quarks of proton FFs. In our analyses, since the gluon and heavy quark parameters γ_g , γ_c and γ_b affect the χ^2 value, we omit the term $[1 - e^{-\gamma z}]$ for these partons to get the best fit. With these assumptions, there are 20 parameters which must be determined by fitting. Our results for the fit parameters at LO and NLO are listed in Tables. I and II. The obtained values of $\chi^2/d.o.f$ for proton at LO and NLO are 1.702 and 1.626 in our global fit, respectively, and in next section we will show that this value can be reduced when one imposes the effect of proton mass into the calculations.

The initial scale μ_0 is different for partons so that the value of $\mu_0^2 = 1 \text{ GeV}^2$ is chosen for splitting of the gluon and light-quarks into the proton and for the c - and b -quarks it is taken to be $\mu_0^2 = m_c^2$ and $\mu_0^2 = m_b^2$, respectively.

According to the partonic structure of the proton, the proton FFs can be applied for the anti-proton as

$$D_i^{\bar{p}}(z, \mu_0^2) = D_i^p(z, \mu_0^2). \quad (7)$$

In Fig. 1, using the proposed functional forms of the proton FFs, we compare our results for $1/\sigma_{tot} \times d\sigma^p/dx_p$ with SIA experimental data at $\mu^2 = M_Z^2$ reported by the ALEPH, SLD and DELPHI collaborations at NLO. In these figures we separate the light, charm and bottom tagged cross sections, and as it is seen most of the diagrams are in a reliable consistency with the experimental data. The NLO proton FFs are presented in Fig. 2 at the initial scales $\mu_0^2 = 1 \text{ GeV}^2$ for the gluon and light quarks and $\mu_0^2 = m_c^2$ and $\mu_0^2 = m_b^2$ for the c - and b -quarks, respectively. In Fig. 3, our results for different flavors are compared with other collaborations at the scale $Q^2 = M_Z^2$, where we have used the DSS set [22] that included electron-positron, lepton-nucleon, and hadron-hadron scattering data, and the HKNS set [23] that included electron-positron data. Note that, as Fig. 1 shows, due to the largeness of the χ^2 contribution for the SLD b-tagged data (see Table. IV) some points are outside of the curves. However, χ^2 -values of the heavy quarks are usually larger than the other data and this

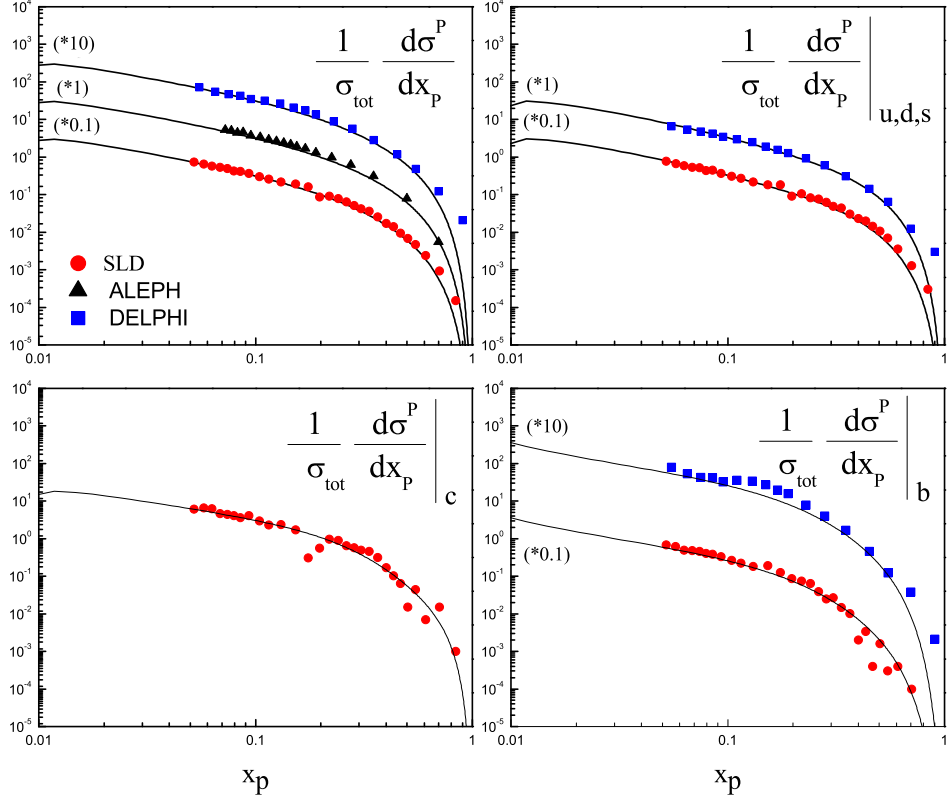


Figure 1: Comparison of our NLO results for $1/\sigma_{\text{tot}} \times d\sigma^P/dx_p$ in total and tagged cross sections with proton production data at $Q^2 = M_Z^2$ by *ALEPH* [24], *DELPHI* [25, 26] and *SLD* [27].

Table I: Values of the fit parameters for the proton FFs at LO in the starting scales.

flavor i	N_i	α_i	β_i	γ_i
u	1.054	-1.532×10^{-5}	2.509	0.501
d	2.946	-1.532×10^{-5}	2.509	0.501
\bar{u}	9.119	-0.225	5.04	0.931
\bar{d}	7.977	-0.225	5.04	0.931
s, \bar{s}	2.832	-0.225	5.04	0.931
c, \bar{c}	4.514	0.704	7.04	...
b, \bar{b}	9.778	0.670	11.596	...
g	1.229	6.455	0.507	...

might be caused to some extent by contaminations from weak decay.

III. PROTON MASS EFFECTS

In this section, we show how to incorporate the hadron mass effects into inclusive hadron production in e^+e^- reaction and into its relevant kinematic variables. The same scheme can be applied for hadron-hadron reactions. To explain our procedure, at first, we review the factorization theorem and its kinematic variables defined. Consider the process

$$e^+e^- \rightarrow Z/\gamma^*(q) \rightarrow a(p_a)\bar{a}(p_{\bar{a}}) \rightarrow H(p_H) + X, \quad (8)$$

where the four-momenta are also shown and $s = q^2$ is the squared of the center-of-mass (c.m.) energy. By ignoring the mass of produced hadron H and outgoing partons a and \bar{a} , in the c.m. frame the momenta take the following form

$$q = (\sqrt{s}, \vec{0}), \quad p_a = (E_a, \vec{0}, E_a), \quad p_H = (E_H, \vec{0}, E_H), \quad (9)$$

where we assumed that the parent partons, i.e. a and \bar{a} , and produced hadrons are emitted in the direction of the 3-axis. Considering the definition of the cross section, one can write

$$d\sigma(x_H, s) = \sum_{a=u,d,s,\dots} \int dz d\hat{\sigma}_a(\mu_R, \mu_F) \Big|_{E_a=E_H/z} D_a^H(z, \mu_F), \quad (10)$$

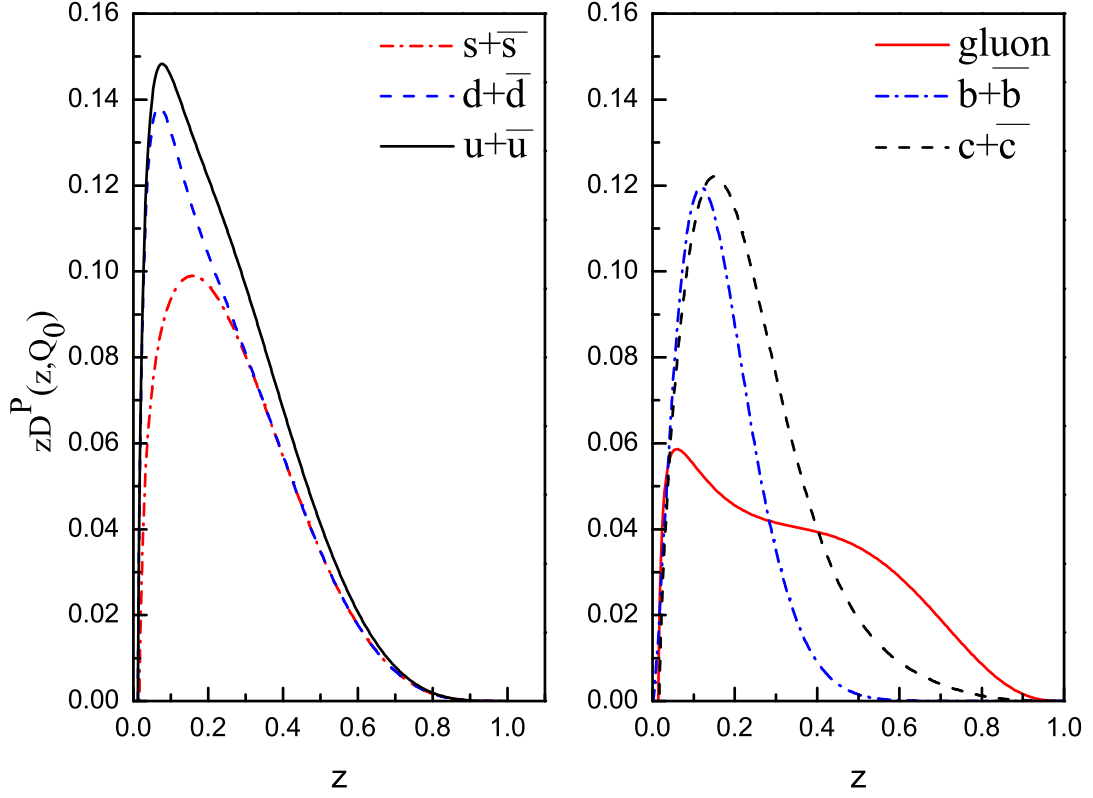


Figure 2: Proton fragmentation functions are shown at $Q_0^2 = 1 \text{ GeV}^2$, m_c^2 and m_b^2 at NLO.

Table II: As in Table. I, but at NLO.

flavor i	N_i	α_i	β_i	γ_i
u	3.206	-0.759	7.935	2.320
d	2.284	-0.759	7.935	2.320
\bar{u}	21.007	-0.533	3.795	0.101
\bar{d}	15.990	-0.533	3.795	0.101
s, \bar{s}	7.999	-0.533	3.795	0.101
c, \bar{c}	6.120	0.826	7.949	...
b, \bar{b}	7.218	0.560	11.617	...
g	3.739	4.290	1.736	...

where $d\hat{\sigma}_a$ are the Wilson coefficients in the parton level (the cross sections for the processes $e^+e^- \rightarrow a\bar{a}$) and D_a^H is the $a \rightarrow H$ FF. Here, $x_H = 2p_H \cdot q/q^2 = 2E_H/\sqrt{s}$ and $z = E_H/E_a$ are the scaling variables. Since the measured observable is $d\sigma/dx_H$, by defining $x_a = 2p_a \cdot q/q^2 = 2E_a/\sqrt{s}$ one can write $d\hat{\sigma}_a = dx_H(dx_a/dx_H)d\hat{\sigma}_a/dx_a$, then

$$\frac{d\sigma}{dx_H}(x_H, s) = \sum_a \int dz \frac{d\hat{\sigma}_a}{dx_a} \frac{dx_a}{dx_H} D_a^H\left(\frac{x_H}{x_a}, \mu_F\right). \quad (11)$$

Considering the definition of $x_a = x_H/z$, one has $dx_a/dx_H = 1/z$ and, therefore, can write $dz/z = -dx_a/x_a$ so that the equation above is simplified to the

following form

$$\frac{d\sigma}{dx_H}(x_H, s) = \sum_a \int_{x_H}^1 \frac{dx_a}{x_a} \frac{d\hat{\sigma}}{dx_a} D_a^H\left(\frac{x_H}{x_a}, \mu_F\right), \quad (12)$$

that leads to the relation (2). In the equation above, one has $\sqrt{\rho_H^2} \leq x_H \leq 1$ where $\rho_H = 2m_H/\sqrt{s}$ is the cut-off and if one sets the hadron mass as $m_H = 0$ then $0 \leq x_H \leq 1$.

Note that, to establish the factorization theorem we ignored the hadron and parton masses when we defined the scaling variables x_H and x_a . To incorporate the hadron mass effects we use a specific choice of scaling variables. For this purpose it is helpful to work with light-cone (L.C) coordinates system, in which any four-vector V is written in the form of $V = (V^+, V^-, \vec{V}_T)$ with

Table III: The individual χ^2 values at the LO for each collaboration and the total χ^2 fit for proton.

Collaboration	data properties	\sqrt{s} GeV	data points	$\chi^2(\text{LO})$ normalization in fit
TPC [28]	untagged	29	8	17.22
TASSO [29]	untagged	34	4	1.910
ALEPH [24]	untagged	91.2	18	22.239
SLD [27]	untagged	91.28	28	75.263
	<i>uds</i> tagged	91.28	29	52.377
	<i>c</i> tagged	91.28	29	41.419
	<i>b</i> tagged	91.28	28	59.895
DELPHI [25, 26]	untagged	91.2	17	3.729
	<i>uds</i> tagged	91.2	17	4.261
	<i>b</i> tagged	91.2	17	16.094
TOTAL: ($\chi^2/\text{d.o.f}$)			195	294.407 1.702

Table IV: As in Table. III, but at NLO.

Collaboration	data properties	\sqrt{s} GeV	data points	$\chi^2(\text{NLO})$ normalization in fit
TPC [28]	untagged	29	8	21.984
TASSO [29]	untagged	34	4	2.143
ALEPH [24]	untagged	91.2	18	19.955
SLD [27]	untagged	91.28	28	83.960
	<i>uds</i> tagged	91.28	29	43.920
	<i>c</i> tagged	91.28	29	39.010
	<i>b</i> tagged	91.28	28	45.795
DELPHI [25, 26]	untagged	91.2	17	4.734
	<i>uds</i> tagged	91.2	17	5.861
	<i>b</i> tagged	91.2	17	13.929
TOTAL: ($\chi^2/\text{d.o.f}$)			195	281.291 1.626

$V^\pm = (V^0 \pm V^3)/\sqrt{2}$ and $\vec{V}_T = (V^1, V^2)$.

Considering the L.C coordinates, the four-momenta of particles in the e^+e^- reaction (9) are expressed as

$$q = (\frac{\sqrt{s}}{\sqrt{2}}, \frac{\sqrt{s}}{\sqrt{2}}, \vec{0}), \quad p_H = (\sqrt{2}E_H, 0, \vec{0}), \quad (13)$$

and $p_a = (\sqrt{2}E_a, 0, \vec{0})$. Therefore, in absence of hadron mass, the scaling $x_H = 2E_H/\sqrt{s}$ is expressed as $x_H = p_H^+/q^+$ in the L.C coordinates. From now on, we define $\eta = p_H^+/q^+$ as the light-cone scaling variable which is identical to the x_H -variable in the absence of hadron mass. The η is now a more convenient scaling variable for studying hadron mass effects since it is invariant with respect to boosts along the direction of the hadron's spatial momentum (Z -axis). Taking a mass m_H for the hadron, the momentum of the hadron in the c.m. frame reads

$$p_H = (p_H^+, p_H^-, \vec{p}_T) = (\eta q^+, p_H^-, \vec{p}_T) = (\eta \frac{\sqrt{s}}{\sqrt{2}}, p_H^-, \vec{0}). \quad (14)$$

With respect to $p_H^2 = m_H^2$ and considering the inner product in the L.C system ($V \cdot V = 2V^+V^- - V_T^2$), the hadron momentum is expressed as

$$p_H = (\eta \frac{\sqrt{s}}{\sqrt{2}}, \frac{m_H^2}{\eta \sqrt{2}s}, \vec{0}). \quad (15)$$

As a generalization of the massless case, we assume that the cross section in the new coordinate system is obtained by the replacements $x_H \rightarrow \eta$ and $x_a \rightarrow y$ in (12), i.e.

$$\frac{d\sigma}{d\eta}(\eta, s) = \sum_a \int_\eta^1 \frac{dy}{y} \frac{d\hat{\sigma}}{dy} D_a^H(\frac{\eta}{y}, \mu_F). \quad (16)$$

Since the experimental quantity is $d\sigma/dx_H$, then it can be related to the $d\sigma/d\eta$ via

$$\frac{d\sigma}{dx_H}(x_H, s) = \frac{d\sigma}{d\eta}(\eta, s) \times \frac{d\eta}{dx_H}. \quad (17)$$

By comparing the hadron momentum in the L.C system, $p_H = ((p_H^0 + p_H^3)/\sqrt{2}, (p_H^0 - p_H^3)/\sqrt{2}, \vec{0})$, with the equation (15), the relation between the two scaling variables is

$$p_H^0 = \frac{1}{2}(\eta\sqrt{s} + \frac{m_H^2}{\eta\sqrt{s}}) \implies x_H = \eta(1 + \frac{m_H^2}{s\eta^2}). \quad (18)$$

Note that these two variables are approximately equal when $m_h \ll x_H\sqrt{s}$. Considering the equation (18), one has

$$\frac{d\eta}{dx_H} = \frac{1}{1 - \frac{m_H^2}{s\eta^2(x_H)}}. \quad (19)$$

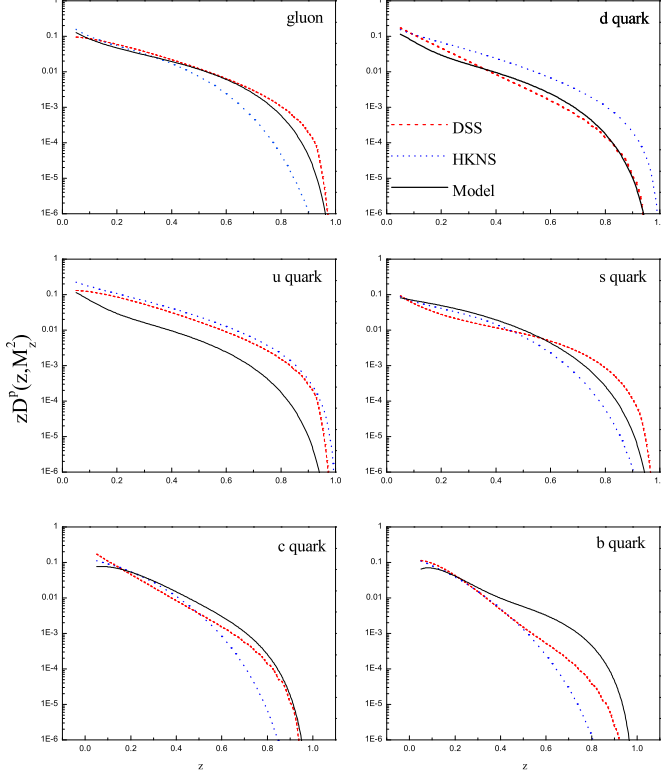


Figure 3: Comparison of extracted proton FFs at $Q^2 = M_Z^2$ with DSS [22] (dashed lines) and HKNS [23] (dotted lines).

Finally, the improved factorization theorem in the presence of hadron mass reads

$$\frac{d\sigma}{dx_H}(x_H, s) = \frac{1}{1 - \frac{m_H^2}{s\eta^2(x_H)}} \frac{d\sigma}{d\eta}(\eta(x_H), s). \quad (20)$$

In Fig. 4, considering the massive and massless protons the FFs of partons at the scale $Q = 34$ GeV are shown. As it is seen, the mass of proton affects the FFs of the gluon and light quarks d and u . In Fig. 5, our results for $1/\sigma_{tot} \times d\sigma^p/dx_p$ are compared with the data from TPC collaborations at $Q = 29$ GeV for the massless and massive protons. In Fig. 6, the same comparison is done at $Q = 34$ GeV. Note that the effect of proton mass is to reduce the size of the cross section at large z which is needed to improve the fit when one works with data from TPC. Our result for the fit parameters in the presence of the proton mass is listed in Table. V. As it is shown in Table. VI the effect of proton mass is to reduce the value of $\chi^2/d.o.f$, which is now 1.583 in our global fit.

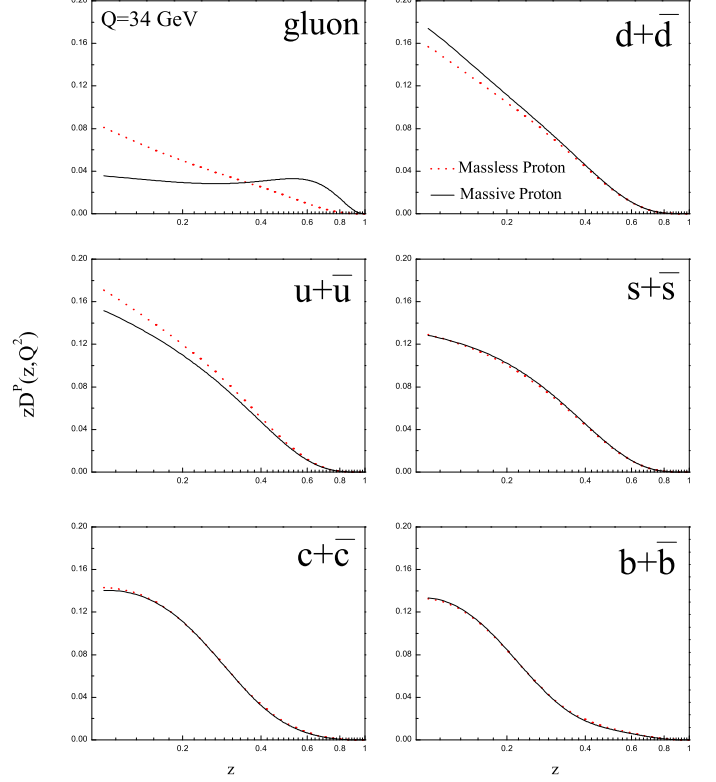


Figure 4: Comparison of NLO proton FFs at $Q = 34$ GeV in massive (solid lines) and massless (dotted lines) proton cases.

Table V: Values of the fit parameters for the proton FFs at NLO, by incorporating mass effects in the fit. We set the proton mass as $m_p = 938.272$ MeV.

flavor i	N_i	α_i	β_i	γ_i
u	2.016	-0.695	16.080	2.314
d	4.676	-0.695	16.080	2.314
\bar{u}	19.005	-0.601	3.665	0.090
\bar{d}	17.984	-0.601	3.665	0.090
s, \bar{s}	8.878	-0.601	3.665	0.090
c, \bar{c}	6.908	0.867	7.967	...
b, \bar{b}	7.560	0.569	11.569	...
g	3.515	4.388	1.739	...

IV. ENERGY SPECTRUM OF THE INCLUSIVE PROTON IN TOP QUARK DECAYS

In the last section, we apply the massive proton FFs to make our phenomenological predictions for the energy spectrum of the proton produced through unpolarized top decays

$$t \rightarrow b + W^+(g) \rightarrow p + X, \quad (21)$$

where X refers to the unobserved final state. Note that, both the bottom quark and the gluon may hadronize into

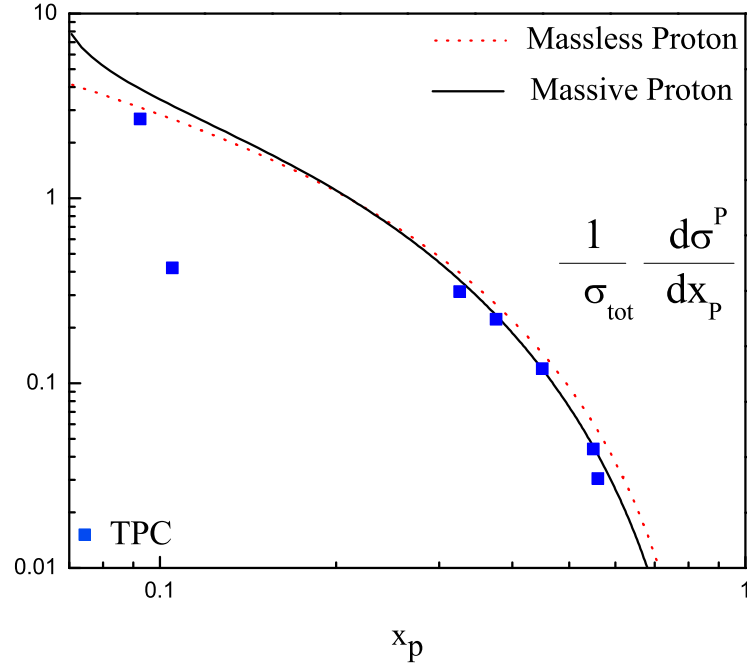


Figure 5: Comparison of our NLO results for the total cross section $1/\sigma_{tot} \times d\sigma/dx_p$ with data from *TPC* [28] at $Q = 29$ GeV. The effect of proton mass is also considered in the solid curve.

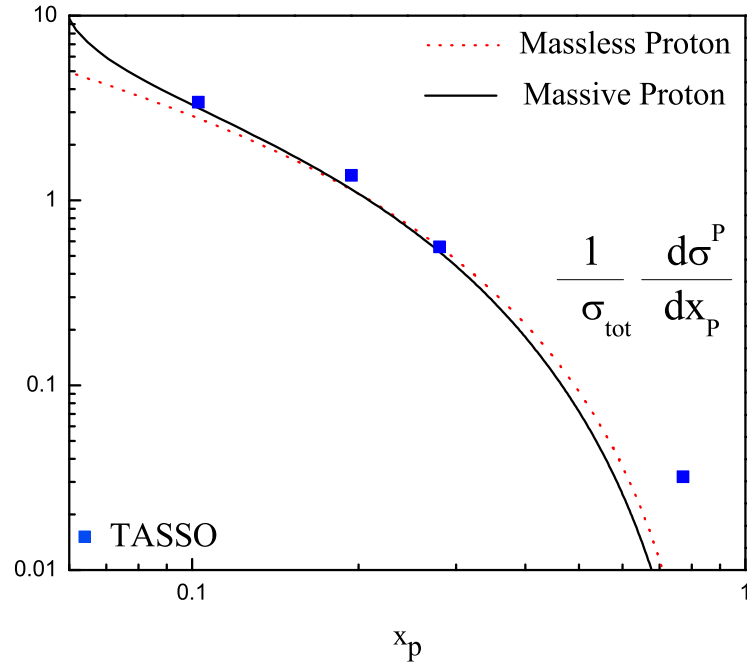


Figure 6: As in Fig. 5, but comparison is done with data from *TASSO* [29] at $Q = 34$ GeV.

the produced proton, so that the gluon contributes to the real radiation at NLO.

Generally, to obtain the energy spectrum of the produced hadron H , we employ the factorization theorem (12),

which is now expressed as

$$\frac{d\Gamma}{dx_H} = \sum_{i=b,g} \int_{x_i^{min}}^{x_i^{max}} \frac{dx_i}{x_i} \frac{d\Gamma}{dx_i}(\mu_R, \mu_F) D_i^H\left(\frac{x_H}{x_i}, \mu_F\right) \quad (22)$$

where, as in [4], we defined the scaled-energy fraction of hadron as $x_H = 2E_H/(m_t^2 - m_W^2)$ and $d\Gamma/dx_i$ are

Table VI: The individual χ^2 values for each collaboration and the total χ^2 fit for proton when incorporating the proton mass.

Collaboration	data properties	\sqrt{s} GeV	data points	$\chi^2(\text{NLO})$ normalization in fit
TPC [28]	untagged	29	8	20.648
TASSO [29]	untagged	34	4	2.118
ALEPH [24]	untagged	91.2	18	18.408
SLD [27]	untagged	91.28	28	83.724
	<i>uds</i> tagged	91.28	29	42.743
	<i>c</i> tagged	91.28	29	38.603
	<i>b</i> tagged	91.28	28	43.927
DELPHI [25, 26]	untagged	91.2	17	4.390
	<i>uds</i> tagged	91.2	17	4.994
	<i>b</i> tagged	91.2	17	14.241
TOTAL:			195	273.796
($\chi^2/\text{d.o.f}$)				1.583

the parton-level differential rates of the process $t \rightarrow i + W^+(i = b, g)$. The NLO analytical expressions for the parton-level differential widths $d\Gamma/dx_i$ are presented in Refs. [3, 4]. The factorization and the renormalization scales are normally arbitrary so, here, we set them as $\mu_R = \mu_F = m_t = 172.9$ GeV. For numerical analysis, we also set $m_b = 4.78$ GeV, $\Lambda^{NLO} = 231$ MeV and $m_W = 80.39$ GeV.

In Fig. 7, our predictions for the proton energy spectrum are shown by studying the contributions of the $(b, g) \rightarrow p$ at NLO. As it is shown, the gluon contribution into the proton (dot-dashed line) is negative and appreciable only in the low x_p region. Note that the contribution of the gluon fragmentation cannot be discriminated and it is calculated to see where it contributes to $d\Gamma/dx_p$. In fact, this part of the plot is of more theoretical relevance. In the energy spectrum of hadrons, all contributions including the b-quark and gluon contribute. In Fig. 7, the total contribution (solid line) at $\mu_F = m_t$ is presented too. In Fig. 8, our prediction for the $d\Gamma(t \rightarrow p + X)/dx_p$ is compared with the result obtained by using the FFs of AKK collaborations [16]. As is seen, there is good consistency between the predictions.

V. CONCLUSION

We determined the new non-perturbative fragmentation functions of proton in the parton model of QCD through a global analysis on SIA data at the LO and NLO approximations. Our new parametrization of the proton FFs covers a wide kinematic range of z , in the

presence of the extra term $(1 - e^{-\gamma_i z})$ which controls the medium- z region and improves the accuracy of the global fit. Fig. 1 represents the comparison of our model with SIA experimental data that shows our model is successful. We determined the FFs of gluon and light quarks at the initial scales $\mu_0^2 = 1$ GeV² and the FFs of heavy quarks at $\mu_0^2 = m_c^2$ and $\mu_0^2 = m_b^2$, so their evaluation was performed by using the DGLAP equations. Our analysis was based on the ZM-VFN scheme, where all partons are treated as massless particles and the non-zero values of the c- and b-quark masses only enter through the initial conditions of the FFs. In comparison with other groups we also considered the effects of proton mass on the FFs and showed that this effect improves the accuracy of the global fit, specifically for the data from SLAC (TPC Collaborations). The proton mass affects the light and gluon FFs while for the heavy quark FFs this effect is less important. The advent of precise data from LHC offers us the opportunity of further constrain the proton FFs and to test their scaling violations. This situation motivates the incorporation of proton mass effects, which are then likely to be no longer negligible, into the formalism. The mass of proton also sets a bound on the scaling variable $x_p \geq 2m_p/\sqrt{s}$.

Finally, as an application we used the computed FFs to study the scaled-energy distribution of the proton in unpolarized top quark decays. At LHC, the energy distribution of hadrons in top decays enables us to deepen our knowledge of the hadronization process. The universality and scaling violations of the proton fragmentation functions will be able to test at LHC by comparing our NLO predictions with future measurements of $d\Gamma/dz$.

Besides NLO corrections, some other corrections can improve our analysis. In next work, we plan to extend the method developed in [38] in the framework of e^+e^- process in which large logarithmic terms, due to soft-gluon radiation, are evaluated and resummed to all perturbative orders in the QCD coupling α_s .

Acknowledgments

We are grateful to Gennaro Corcella for his careful reading of the manuscript and also for constructive discussions and comments. We would also like to thank Bernd A. Kniehl and the DESY theoretical division for their hospitality, where a portion of this work was performed.

-
- [1] D. P. Anderle, F. Ringer and M. Stratmann, arXiv:1510.05845 [hep-ph].
 - [2] S. M. M. Nejad, Phys. Rev. D **88**, no. 9, 094011 (2013).
 - [3] B. A. Kniehl, G. Kramer and S. M. Moosavi Nejad, Nucl. Phys. B **862** (2012) 720.

- [4] G. Corcella and A. D. Mitov, Nucl. Phys. B **623**, 247 (2002).
- [5] CMS Collaboration [CMS Collaboration], CMS-PAS-TOP-15-002.
- [6] G. Corcella, arXiv:1511.08429 [hep-ph].

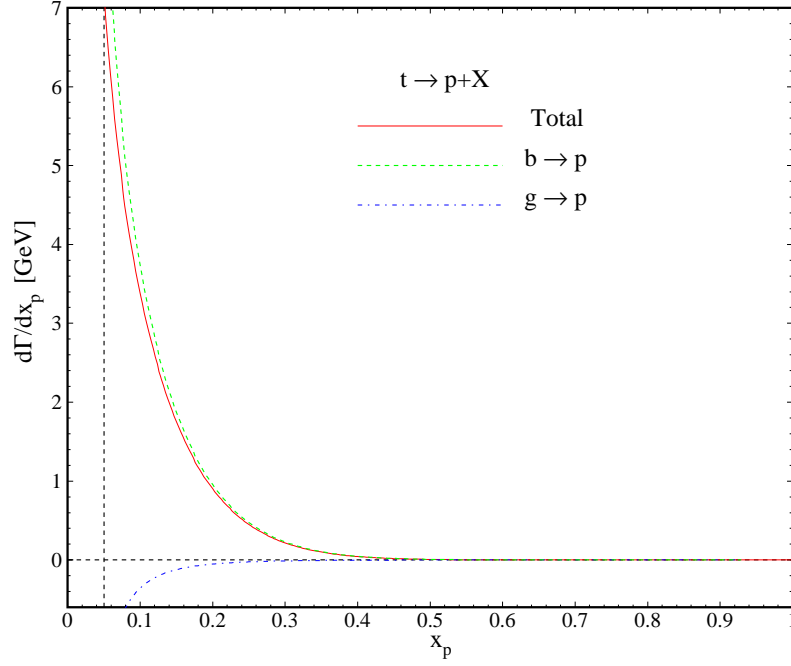


Figure 7: $d\Gamma(t \rightarrow p + X)/dx_p$ as a function of x_p (solid line) at $\mu_F = m_t$. The NLO result is broken up into the contributions due to $b \rightarrow p$ (dashed line) and $g \rightarrow p$ (dot-dashed line) fragmentations.

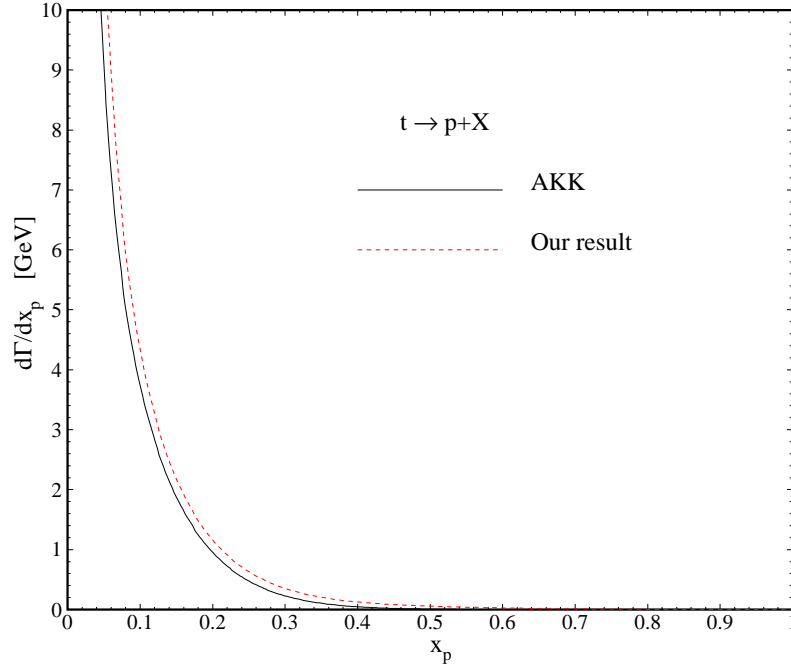


Figure 8: Our result for the partial decay rate is shown using the extracted $(b, g) \rightarrow p$ FFs in presence of proton mass. To compare we also show the same distribution using the FFs presented by AKK [16].

- [7] J. P. Ma, Nucl. Phys. B **506** (1997) 329.
- [8] E. Braaten and T. C. Yuan, Phys. Rev. Lett. **71** (1993) 1673.
- [9] J. D. Bjorken, Phys. Rev. D **17** (1978) 171.
- [10] C. Peterson, D. Schlatter, I. Schmitt and P. M. Zerwas, Phys. Rev. D **27** (1983) 105.
- [11] M. Suzuki, Phys. Lett. B **71** (1977) 139.
- [12] F. Amiri and C. -R. Ji, Phys. Lett. B **195** (1987) 593.
- [13] S. M. M. Nejad and A. Armat, Eur. Phys. J. Plus **128** (2013) 121.
- [14] S. M. Moosavi Nejad, Eur. Phys. J. Plus **130** (2015) 7, 136; S. M. M. Nejad and M. Delpasand, Int. J. Mod.

- Phys. A **30** (2015) 1550179.
- [15] F. Arbabifar, A. N. Khorramian and M. Soleymaninia, Phys. Rev. D **89**, no. 3, 034006 (2014).
 - [16] S. Albino, B. A. Kniehl and G. Kramer, Nucl. Phys. B **803**, 42 (2008).
 - [17] E. Leader, A. V. Sidorov and D. B. Stamenov, arXiv:1506.06381 [hep-ph].
 - [18] D. de Florian, R. Sassot, M. Epele, R. J. Hernandez-Pinto and M. Stratmann, Phys. Rev. D **91** (2015) 1, 014035.
 - [19] M. Soleymaninia, A. N. Khorramian, S. M. Moosavi Nejad and F. Arbabifar, Phys. Rev. D **88**, no. 5, 054019 (2013) [Phys. Rev. D **89**, no. 3, 039901 (2014)].
 - [20] M. Soleymaninia, A. N. Khorramian, S. M. Moosavi Nejad and F. Arbabifar, Acta Phys. Polon. Supp. **7**, no. 3, 573 (2014). doi:10.5506/APhysPolBSupp.7.573
 - [21] D. de Florian, R. Sassot and M. Stratmann, Phys. Rev. D **75**, 114010 (2007).
 - [22] D. de Florian, R. Sassot and M. Stratmann, Phys. Rev. D **76**, 074033 (2007).
 - [23] M. Hirai, S. Kumano, T. -H. Nagai and K. Sudoh, Phys. Rev. D **75**, 094009 (2007).
 - [24] D. Buskulic *et al.* (ALEPH collaboration), Z. Phys. **C66**, 355 (1995); R. Barate *et al.*, Phys. Rep. **294**, 1 (1998).
 - [25] P. Abreu *et al.* (DELPHI collaboration), Eur. Phys. J. **C5**, 585 (1998).
 - [26] P. Abreu *et al.* (DELPHI collaboration), Nucl. Phys. **B444**, 3 (1995).
 - [27] K. Abe *et al.* (SLD collaboration), Phys. Rev. **D69**, 072003 (2004).
 - [28] H. Aihara *et al.* (TPC collaboration), Phys. Rev. Lett. **52**, 577 (1984); **61**, 1263 (1988).
 - [29] W. Braunschweig *et al.* (TASSO collaboration), Z. Phys. **C42**, 189 (1989).
 - [30] J. C. Collins, Phys. Rev. D **58** (1998) 094002.
 - [31] V. N. Gribov and L. N. Lipatov, Sov. J. Nucl. Phys. **15**, 438 (1972) [Yad. Fiz. **15**, 781 (1972)]; G. Altarelli and G. Parisi, Nucl. Phys. **B126**, 298 (1977); Yu. L. Dokshitzer, Sov. Phys. JETP **46**, 641 (1977) [Zh. Eksp. Teor. Fiz. **73**, 1216 (1977)].
 - [32] T. Kneesch, B. A. Kniehl, G. Kramer and I. Schienbein, Nucl. Phys. B **799**, 34 (2008).
 - [33] S. Kretzer, Phys. Rev. D **62**, 054001 (2000).
 - [34] B. A. Kniehl and G. Kramer, Phys. Rev. D **71**, 094013 (2005).
 - [35] J. Binnewies, B. A. Kniehl and G. Kramer, Z. Phys. C **65**, 471 (1995).
 - [36] B. A. Kniehl, G. Kramer, I. Schienbein and H. Spiesberger, Phys. Rev. D **77**, 014011 (2008).
 - [37] B. R. Webber, Nucl. Phys. B **238** (1984) 492.
 - [38] M. Cacciari and S. Catani, Nucl. Phys. B **617** (2001) 253 doi:10.1016/S0550-3213(01)00469-2.